Compact Multilayer Dual-mode Substrate Integrated Waveguide Filtering Crossover Based on Orthogonal Modes

Zhigang Zhang and Yong Fan

Fundamental Science on Extreme High Frequency Key Laboratory
University of Electronic Science and Technology of China, Chengdu 611731, China
freemanzzg@163.com, yfan@uestc.edu.cn

Abstract ─ A novel multilayer substrate integrated waveguide (SIW) filtering crossover is proposed based on the orthogonal degenerate modes in SIW rectangular cavities (SIRCs). The degeneracy of dual-mode in multilayer SIRCs is used to realize the cross transmission and the orthogonality of the two modes is utilized to achieve the isolation relying on the four coupling slots located on metal layers. E-field distributions of the SIW cavities at TE_{102} and TE_{201} modes are studied for guiding the circuit realization. And then input/output and isolated ports can share the same resonator, which reduces the number of resonators by two. By adjusting the position of the coupling slots located between layers, the bandwidth can be controlled independently in a certain range without affecting the isolation effect. The detailed analysis and the design method based on coupling matrix have been first introduced to realize a third-order multilayer filtering crossover. Compared with other filtering crossovers, the proposed design exhibits good filtering responses, better isolation, lower loss, as well as compact size.

Index Terms ─ Dual-mode, filtering crossover, multilayer, and substrate integrated waveguide (SIW).

I. INTRODUCTION

Crossovers are essential components in various microwave and millimeter-wave circuits, which allow different signals to cross each other without mutual interferences. It can be applied in the Butler matrix which has been widely used to construct modern beam-forming technology. However, most of these crossovers are implemented by microstrip technology, which would always suffer from high losses in high frequency-band.

To meet the need of higher frequency operation, the emerging substrate-integrated waveguide (SIW) technology [1-8] has been successfully applied to the design of various crossovers with high isolation, low insertion, and easy integration with other planar circuits. Moreover, a variety of microwave filters [1,5-6], power dividers [2,7], couplers, and antennas [3] are well designed based on SIW structures.

Since the conventional SIW circuits are still too large for high-density microwave/millimeter wave systems, miniaturization design is becoming one of the primary trends for SIW components. The use of multilayered topologies [4-6] is known to provide more freedom to design coupling paths between waveguided structures while maintaining a compact circuit size. A compact multilayer dual-mode filter based on the substrate integrated waveguide circular cavity (SICC) is developed in [5]. A novel out-of-phase power divider based on a two-layer SIW is presented in [8].

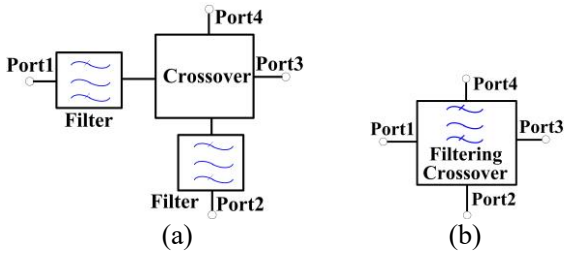

Fig. 1. Schematic of the crossover cascaded with BPFs and the filtering crossover: (a) traditional crossover; (b) filtering crossover.

As shown in Fig. 1, two filters are needed to integrate bandpass responses to one crossover, occupying large circuit areas. To further reduce size, a single device integrated with different functionalities, such as filtering crossover [9-16] has been attracting increasing attention. It also recommends an effective method to avoid the interstage mismatch and performance degradation due to a cascade connection of two individual components. A wideband filtering crossover using dual-mode ring resonator is proposed in [9]. In [12], a compact crossover with bandpass responses is presented by using a stub-loaded ring structures. In [16], a SIW filtering crossover is proposed based on degenerate modes in SIW cavities. Nevertheless, the footprint of this crossover is a little large due to the employment of five oversized square

Submitted On: January 7, 2020
Accepted On: April 4, 2020

cavities. As for aforementioned filtering crossover [13-16], the bandwidth can be adjusted only by changing the size of coupling aperture, which will also affect isolation level at the same time.

In this paper, a compact multilayer dual-mode SIW filtering crossover is presented based on the orthogonal degenerate modes in SIW rectangular cavities (SIRCs). The main design concept of this crossover is to make full use of the dual-modes in multilayer SIW rectangular cavities (SIRCs) to realize the cross transmission and the orthogonality of the two modes to achieve the isolation relying on the four coupling slots located between substrate layers. Unlike other filtering crossovers [9-12, 16] (each port need to be loaded a resonator), by utilizing the isolation property of the orthogonal degenerate modes, input/output and isolated ports can share the same resonator, which reduces the number of resonators by two. Moreover, with multilayer dual-mode technology, a third-order filtering crossover with flexibly controlled bandwidth can be realized by occupying only one resonator area. Comparatively speaking, both the bandwidth and isolation level of planar filtering crossover [12-16] depends on the width of the coupling aperture. By adjusting the position of the four coupling slots located between layers, the bandwidth of proposed design can be controlled independently in a certain range without affecting the isolation effect. What's unique about the analysis process of crossover is that the filtering crossover is divided into two band-pass filters (BPFs), and then the coupling matrix method is used to evaluate the initial value of design parameters accurately according to the specifications, which is beneficial to accelerate the later optimization design process. It's a good combination of multilayered topologies, dual-mode SIW cavities and multifunctional components [18-24], which realize the miniaturization design of the device while keeping good performance.

II. ANALYSIS AND DESIGN

A. Filtering crossover structure

As shown in Fig. 2, the proposed filtering crossover consists of three SIW rectangular cavities (SIRCs), which are coupled with each other by the four rectangular coupling slots located in different layers for miniaturization. Based on the isolation property of the orthogonal degenerate modes, Port1, Port2, and Port3, Port4 share the same Cavity I and III, which save the number of resonators by two. There are two paths for signal transmission (Port1 to 3 and Port2 to 4). When Port1 is the input port, Port3 is the through port, whereas Ports 2 and 4 are isolation port. Since the structure is completely symmetrical, it can be inferred that the signal will only be transmitted from Port 2 to 4 when Port 2 is excited. The coupling slots have variable lengths (*L*slot), widths (*W*slot) and offsets, and are arranged with respect to bandwidth and isolation level. In these figures, *W*c is the width of the external coupling aperture and *L*gap is the length of feeding slot. *L*c1 and *W*c1 are length and width of Cavity I and III. The length and width of Cavity II are denoted as *L*c2 and *W*c2, respectively.

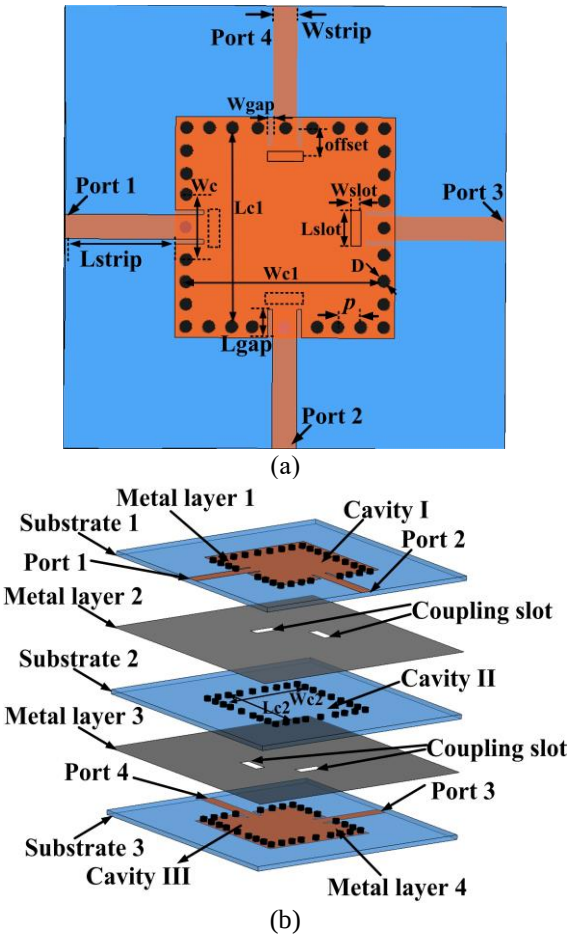

Fig. 2. The proposed multilayer dual-mode SIW filtering crossover: (a) top view; (b) anatomy view.

B. Dual-mode theory

A dual-mode SIW cavity[25-28] can support two degenerate modes within one resonant unite, which not only reduces the circuit size more than half but also adds the design flexibility.

By using the electromagnetic simulation software, the E-field distributions of the square cavity at the orthogonal degenerate modes can be analyzed. Figure 3 depicts the electric field magnitude distributions of TE_{102} and TE_{201} modes in a SIRC. As seen in Fig. 3 (a), the electric field within the SIW cavity is divided into two regions, which are represented as region A and region B. As can be seen, the electric field of TE_{102} mode is the strongest in region A, but the weakest in region B. Compared to the TE_{102} mode, it can be observed the electric field of TE_{201} mode is the weakest in region A, but the strongest in region B, as shown in Fig. 3 (b).

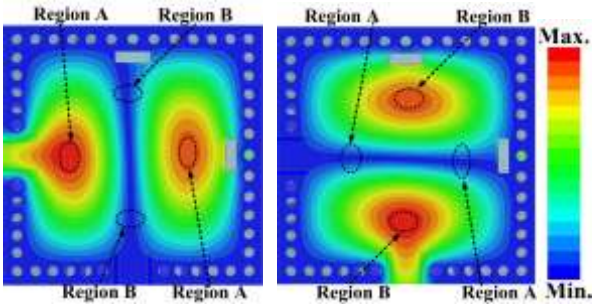

(a) (b)

Fig. 3. E-field distributions of the dual-mode SIW cavity at: (a) TE_{102} mode; (b) TE_{201} mode in SIRC.

Therefore, TE_{102} and TE_{201} modes are orthogonal degenerate modes, which mean that the TE_{102} mode will be driven without the excitation of TE_{201} if the two ports are placed in region A, and vice versa in region B. Given this characteristic, input/output and isolated ports can share the same cavity, which helps to save the number of resonators by two. On the other hand, the resonant frequency of the TE_{m0n} mode for rectangular cavity is decided by [31]:

$$f_{m0n} = \frac{c}{2\sqrt{\mu_r \varepsilon_r}} \sqrt{\left(\frac{m}{a_{eff}}\right)^2 + \left(\frac{n}{b_{eff}}\right)^2}, \tag{1}$$

$$a_{eff} = a - \frac{D^2}{0.95p},\ b_{eff} = b - \frac{D^2}{0.95p}. \tag{2}$$

Where, a_{eff} and b_{eff} are the SIRC's equivalent length, width, respectively. a and b are physical length and width of SIW cavity, D and p are the diameter of metallized via-holes and center-to-center pitch between two adjacent via-holes.

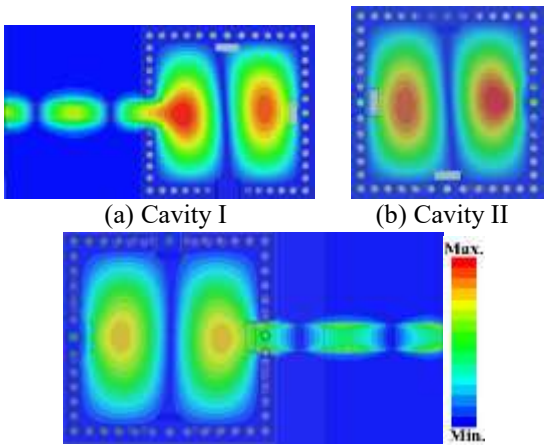

(a) Cavity I (b) Cavity II

(c) Cavity III

Fig. 4. E-field distributions in the multilayer SIW filtering crossover when Port 1 is excited.

Figure 4 illustrates the electric field magnitude distributions at 18 GHz in the multilayer SIW filtering crossover when Port 1 is driven. As can be seen, TE_{102} modes in cavities I~III have been excited to transmit the signal from Port 1 to 3 with the isolation of energy to Ports 2 and 4.

C. Analysis of crossover

The topology of the filtering crossover is shown in Fig. 5 (a). Resonator1, 4, resonator 2, 5 and resonator 3, 6 represent two degenerate modes exist in the same cavity. Since these two modes are perpendicular to each other, there is no coupling between them (M14=M25=M36=0).

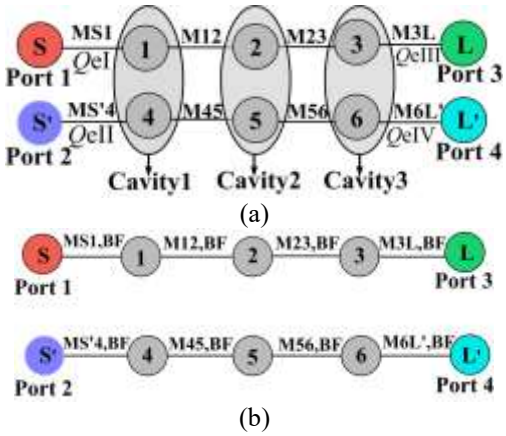

Fig. 5. (a) Topology of the third-order filtering crossover; (b) schematic topology of two third-order filters.

Obviously, there are two paths for signal transmission (Port1 to 3 and Port2 to 4).As depicted in Fig. 5 (b), in these two working states, the filtering crossover is equivalent to two third-order bandpass filters (BPFs) which have the same operating frequency and passband characteristics. The coupling matrix of third-order coupled-resonator BPFs is expressed as:

$$m_{N+2} = \begin{array}{c} \\ S \\ 1 \\ 2 \\ 3 \\ L \end{array} \begin{array}{c} \begin{array}{ccccc} S & 1 & 2 & 3 & L \end{array} \\ \begin{bmatrix} 0 & m_{S1,BF} & 0 & 0 & 0 \\ m_{1S,BF} & 0 & m_{12,BF} & 0 & 0 \\ 0 & m_{21,BF} & 0 & m_{23,BF} & 0 \\ 0 & 0 & m_{32,BF} & 0 & m_{3L,BF} \\ 0 & 0 & 0 & m_{L3,BF} & 0 \end{bmatrix} \end{array}. \tag{3}$$

And the normalized input impedance of the filtering crossover in Fig. 5 (a) is required to be the same as matrix (3). Thus, the coupling coefficients for the filtering crossover topology in Fig. 5 (a) are determined as:

$$M_{S1,BF}=M_{S1},\ M_{S'4,BF}=M_{S'4}, \tag{4a}$$

$$M_{3L,BF}=M_{3L},\ M_{6L',BF}=M_{6L'}, \tag{4b}$$

$$M_{12,BF}=M_{45,BF}=M_{12}=M_{45}, \tag{4c}$$

$$M_{23,BF}=M_{56,BF}=M_{23}=M_{56}, \tag{4d}$$

The required normalized coupling coefficient (m) and external quality factors (Q_e) for the filtering crossover can be calculated by:

$$m_{12} = \frac{M_{12}}{FBW} = \frac{M_{45}}{FBW} = m_{12,BF}\,, \tag{5}$$

$$m_{23} = \frac{M_{23}}{FBW} = \frac{M_{56}}{FBW} = m_{23,BF}\,, \tag{6}$$

$$Q_e = \frac{FBW}{M_{S1}^2} = \frac{FBW}{M_{3L}^2} = \frac{1}{FBW \times m_{S1}^2} = \frac{1}{FBW \times m_{3L}^2}\,. \tag{7}$$

Generally, external quality factor (Qe) is related to the length of feeding slot (Lgap) and the width of external coupling aperture (Wc). It should be noted that Lgap can be used to control the bandwidth, which also have decisive impact on isolation levels. This is mainly because the degenerate mode in another channel will be excited easily for larger Lgap, so the isolation level will decrease with the increase of bandwidth.

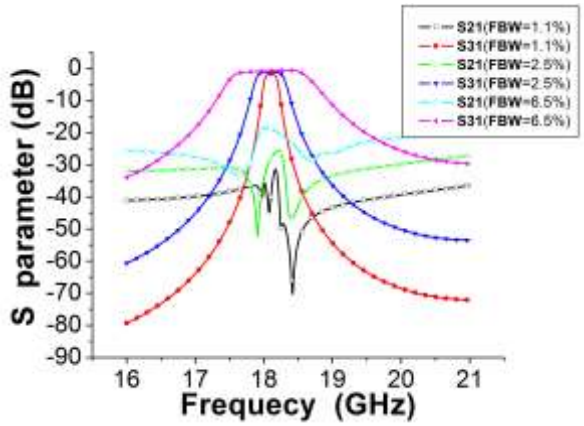

Fig. 6. Simulated S21 and S31 of the proposed third-order multilayer SIW filtering crossover with 25-dB RL and different FBWs

Figure 6 shows the simulated results of the proposed multilayer SIW filtering crossover with the same 25-dB return loss (RL) and different fractional bandwidths (FBWs). It can be seen that the isolation level degrades from −33 to −20 dB when the 3-dB FBW increases from 1.1% to 6.5%.

As for traditional filtering crossover, the bandwidth can be adjusted only by changing the size of coupling aperture, which will also affect isolation level at the same time. Thanks to the multilayer coupling structure, the bandwidth of proposed design can be adjusted independently in a certain range by controlling the position of the coupling slots ($o$ffset), without affecting the isolation effect.

Figure 7 depicts the simulated S-parameter of the proposed multilayer SIW filtering crossover with the same 25-dB isolation level and different fractional bandwidths (FBWs). Obviously, for different FBWs, the isolation level remains unchanged, so the bandwidth of proposed filtering crossover can be adjusted independently. The main reason is that the change of the coupling slots offset only affect the strength of the magnetic coupling, but not stimulate the degenerate mode in another channel.

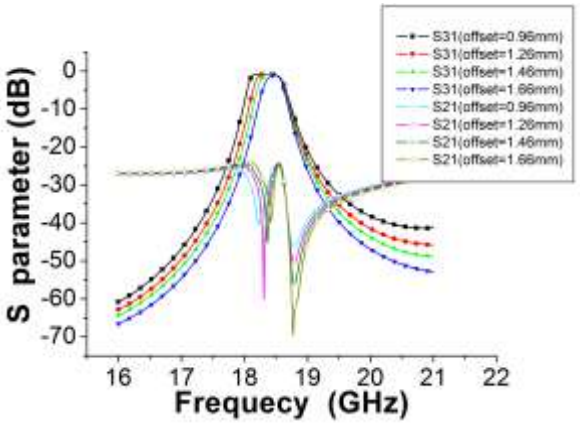

Fig. 7. Simulated S21 and S31 of the proposed third-order SIW filtering crossover with 25-dB isolation level and different FBWs

E. Design example

In our design, the desired passband is centered at 18.2 GHz with the 1.3% fractional bandwidth (FBW) of 25-dB equal-ripple return loss. Based on the advanced coupling matrix synthesis method in [30], the initial normalized coupling matrix of corresponding BPF can be synthesized as:

$$m_{N+2} = \begin{array}{c} \\ S \\ 1 \\ 2 \\ 3 \\ L \end{array} \begin{array}{c} \begin{array}{ccccc} S & 1 & 2 & 3 & L \end{array} \\ \begin{bmatrix} 0 & 1.2214 & 0 & 0 & 0 \\ 1.2214 & 0 & 1.2197 & 0 & 0 \\ 0 & 1.2197 & 0 & 1.2197 & 0 \\ 0 & 0 & 1.2197 & 0 & 1.2214 \\ 0 & 0 & 0 & 1.2214 & 0 \end{bmatrix} \end{array}. \tag{8}$$

From (3)–(8) the desired parameters of the filtering crossover can be calculated as follows:

M_{12}= M_{23}= M_{45}= M_{56}=0.015856, Qe,$_{S1}$=51.5645, Qe,$_{3L}$= Qe,$_{6L}$=51.5645.

To extract Qe, full-wave simulations using ANSYS HFSS are carried out for the singly loaded SIRC excited by a 50-Ω microstrip line. The coupling strengths are controlled by the feeding slot length Lgap with fixed slot width Wgap = 0.3mm and coupling window width Wc = 3.28 mm. Qe can be extracted from the phase and the group delay response of S11 using [29]:

$$Qe = \frac{f_0}{\Delta f_{\pm 90^\circ}}\,. \tag{9}$$

Where, f_0 denotes the frequency at which the group delay

of S11 reaches the maximum, $\Delta f_{\pm 90^\circ}$ indicates the ABW (absolute bandwidth) between ±90° points with respect to the absolute phase of S11 at f_0.

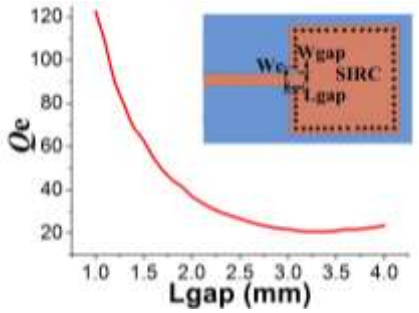

Fig. 8. Simulated external quality factor *Q*e change with *L*gap.

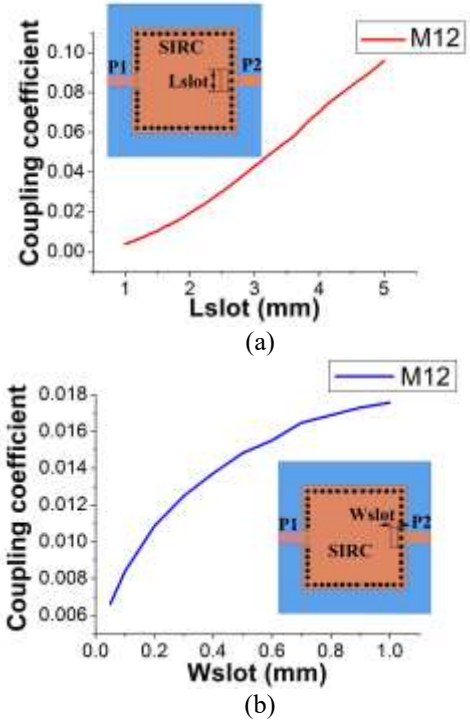

Fig. 9. Coupling coefficients versus the coupling slot: (a) M_{12} versus *L*slot, *W*slot=0.6mm; (b) M_{12} versus *W*slot, *L*slot=1.8mm.

Figure 8 shows the external quality factor *Q*e versus the length of feeding slot *L*gap. It can be seen that the larger the feeding slot length, the smaller the external quality factor. Based on the previous analysis, the filtering crossover can be divided into two bandpss filters. The adjustment of external quality factor is realized by changing the value of *L*gap, as depicted in Fig. 8. Then, the desired *Q*e (*Q*eI = *Q*eII = *Q*e) can be achieved and then the initial value of *L*gap can also be determined.

In general, the coupling coefficient of two coupled resonators can be extracted by full-wave simulations. For two synchronously tuned coupled resonators weakly coupled by input and output ports, two split resonant frequencies can easily be identified by two resonance peaks, the coupling coefficient can then be evaluated using the formula [29]:

$$M_{ij} = \frac{f_{p2}^2 - f_{p1}^2}{f_{p2}^2 + f_{p1}^2}, \tag{10}$$

where f_{p1} and f_{p2} are the lower and higher resonant frequencies, respectively.

Figure 9 illustrates the extracted curves of M_{21}, which versus the length (*L*slot) and width (*W*slot) of coupling slot, respectively. As can be seen, when the length and width of the coupling slot increases, coupling coefficients also increases accordingly. Obviously, larger *L*slot and *W*slot correspond to the wider bandwidth.

In summary, the design procedure of the proposed filtering crossover is listed as follows. Firstly, the resonant frequency of the SIRC is calculated by formula (1) ~ (2), to meet the required center frequency f_0. Secondly, a coupling matrix of a third-order BPF is synthesized according to the desired center frequency f_0 and the fractional bandwidth (FBW). Thirdly, according to formula (3) ~ (8), the coupling matrix and *Q*e of the corresponding filtering crossover are obtained. Moreover, internal coupling parameters (*L*slot, *W*slot, *o*ffset) and external coupling parameters (*W*c, *L*gap) are tuned to meet desired values of coupling coefficients and external quality factor, respectively. Finally, fine tuning of the entire structure is performed to realize good filtering crossover performance.

III. SIMULATED AND MEASURED RESULTS

After optimization implemented by HFSS, the geometry parameters of the proposed filtering crossover are chosen as follows (all in mm): *D*=0.6, *p*=1, *L*c1=*W*c1=12.48, *L*c2=*W*c2=12.61, *L*gap=1.55, *L*slot=1.75, *W*slot=0.6, *W*gap=0.3, *W*strip=1.55, *L*strip=11, *W*c=3.28, *o*ffset=0.95.

To verify the above method ,the proposed crossover was designed and fabricated on a substrate with thickness of 0.508 mm, relative dielectric constant of 2.2 and dielectric loss tangent 0.0009 (at 10 GHz). The measurement is accomplished by using the Agilent N5244A network analyzer.

Figure 10 shows the simulated and measured S-parameters of the multilayer filtering crossover. The measured passband is centered at 18.16 GHz with the 3-dB FBW of 2.35%.The in-band return loss (RL) is better than 19.56dB. The minimum insertion loss (IL) measured in the passband is 1.85 dB, while the isolation is better than 24.5 dB over the band of interest. It could be observed that the measured results are in excellent agreement with the simulation results.

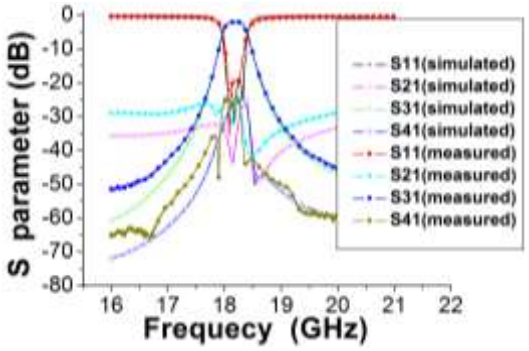

Fig. 10. Simulated and measured results of the fabricated multilayer SIW filtering crossover.

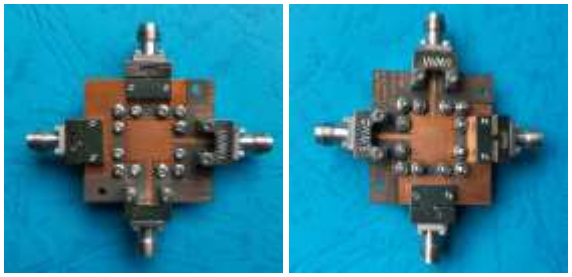

(a) (b)

Fig. 11. Photograph of the fabricated multilayer dual-mode filtering crossover: (a) front view; (b) back view.

Table 1: Performance comparison of various crossovers

Ref.	**f_0(GHz)/ FBW (%)**	**Size(λ_g^2)/ Isolation(dB)/ IL(dB)**	**Techniques/ Resonators*/ RL(dB)/ε_r**
[12]	2/9.5	0.18/20/1.7	Microstrip/ 5/13/3.38
[13]	60/5	1.44/20/0.85	SIW/-/13/9.8
[14]	35/16.6	17.76/17/0.95	SIW/-/17/2.94
[15]	30/2.4	1.44/17/2.2	SIW/5/13/2.2
[16]	20/ 6.6	4.06/20/1.63	SIW/5/18/2.2
[17]	30/16.7	1.44/18/2.1	SIW/5/14/2.2
This work	18.16/2.35	0.69/24.5/1.85	SIW/3/20/2.2

Where λg is the guided wavelength on the substrate at the center frequency f_0, FBW represents the fractional bandwidth. Resonators* represents the number of resonators.

The photograph of the fabricated filtering crossover based on multilayer dual-mode SIRCs is displayed in Fig. 11. A detailed performance comparison with crossovers in recent years is shown in Table 1, which demonstrates the advantages of the proposed crossover clearly. Compared with [12], the proposed design has much higher Q factor and self-consistent electromagnetic shielding structure, which is suitable for higher frequency operation. Moreover, the proposed third-order filtering crossover with flexibly controlled bandwidth can be realized by occupying only one resonator area.

Compared with the works in [13-17], the presented filtering crossover has featured better isolation and RL, flexibly controlled bandwidth, lower loss, minimum number of resonators, as well as more compact size.

IV. CONCLUSION

In this paper, a compact multilayer dual-mode SIW filtering crossover is proposed based on the orthogonal modes in SIRCs. By properly arranging the feeding ports and the four coupling slots in multilayer dual-mode SIRCs, excellent transmission and isolation responses have been successfully achieved. Moreover, input/output and isolated ports can share the same cavity, which save the number of resonators by two. The bandwidth of proposed design can be controlled independently in a certain range without affecting the isolation effect. What's unique about the analysis process of crossover is that the filtering crossover is divided into two band-pass filters (BPFs), and then the coupling matrix method is introduced to evaluate the initial value of design parameters accurately. With the acceptable isolation levels (>20dB), the controllable bandwidth range is from 1.1% to 6.5%. A third-order multilayer filtering crossover operating at 18.2 GHz with a FBW of 2.4% was designed and fabricated. Good circuit performance in the experimental results has verified the proposed ideas. The presented multilayer filtering crossover with dual-mode SIW cavities could be more suitable for the development of high density and miniaturized RF/microwave system.

ACKNOWLEDGMENT

This work was supported in part by the Ministry of Science and Technology of the People's Republic of China under Grant 2013YQ200503 and in part by the National Natural Science Foundation of China (NSFC) under Grant 61001028.

REFERENCES

[1] X.-P. Chen and K. Wu, "Substrate integrated waveguide cross-coupled filter with negative coupling structure," *IEEE Trans. Microw. Theory Tech.*, vol. 56, no. 1, pp. 142-149, Jan. 2008.

[2] K. Song and Q. Xue, "Novel ultra-wideband (UWB) multilayer slotline power divider with bandpass response," *IEEE Microw. Wirel. Compon. Lett.*, vol. 20, no. 1, pp. 13-15, Jan. 2010.

[3] Y. J. Cheng, W. Hong, and K. Wu, "94 GHz substrate integrated monopulse antenna array," *IEEE Trans. Antennas Propag.*, vol. 60, no. 1, pp. 121-128, Jan. 2012.

[4] Y. J. Cheng, W. Hong, K. Wu, and Y. Fan, "A hybrid guided-wave structure of half mode substrate integrated waveguide and conductor-backed slotline and its application in directional

couplers," *IEEE Microw Wireless Compon Lett*. vol. 21, no. 2, pp. 65-67, Feb. 2011.

[5] Z.-G. Zhang, Y. Fan, Y. J. Cheng, and Y.-H. Zhang "A compact multilayer dual-mode substrate integrated circular cavity (SICC) filter for X-band application," *Prog. Electromagn. Res*., vol. 122, no. 1, pp. 453-465, Jan. 2012.

[6] Z.-G. Zhang, Y. Fan, and Y.-H. Zhang, "Compact 3-D multilayer substrate integrated circular and elliptic cavities (SICCs and SIECs) dual-mode filter with high selectivity," *Appl. Comp. Electro. Society (ACES) Journal*, vol. 28, no. 4, pp. 333-340, Apr. 2013.

[7] M.-K. Li, C. Chen, and W. Chen, "Miniaturized dual-band filter using dual-capacitively loaded SIW cavities," *IEEE Microw. Wireless Compon. Lett*., vol. 27, no. 4, pp. 344-346, Apr. 2017.

[8] Q. Chen and J. Xu, "Out-of-phase power divider based on two-layer SIW," *Electron Lett*., vol. 50, no. 14, pp. 1005-1007, July 2014.

[9] W. J. Feng, Y. Zhang, and W. Q. Che, "Wideband filtering crossover using dual-mode ring resonator," *Electron Lett*., vol. 52, no. 7, pp. 541-542, Apr. 2016.

[10] M. Luo, X.-H. Tang, D. Lu, and Y.-H. Zhang, "Approach for filtering crossover design using mixed electric and magnetic coupling," *Electron Lett*., vol. 54, no. 9, pp. 5760-578, May 2018.

[11] Q.-Y. Guo, X. Y. Zhang, and L. Gao, "Novel compact planar crossover with bandpass response based on cross-shaped resonator," *IEEE Trans. Compon., Packag., Manuf. Technol*., vol. 7, no. 12, pp. 2018-2026, Dec. 2017.

[12] X. Y. Zhang, Q.-Y. Guo, K.-X. Wang, B.-J. Hu, and H. L. Zhang, "Compact filtering crossover using stub-loaded ring resonator," *IEEE Microw. Wireless Compon. Lett*., vol. 24, no. 5, pp. 327-329, May 2014.

[13] T. Djerafi and K. Wu, "60 GHz substrate integrated waveguide crossover structure," *in Proc. 39th Eur. Microw. Conf*., Rome, Italy, pp. 1014-1017, 2009.

[14] A. B. Guntupalli, T. Djerafi, and K. Wu, "Ultra-compact millimeter wave substrate integrated waveguide crossover structure utilizing simultaneous electric and magnetic coupling," *in IEEE MTT-S Int. Microw. Symp. Dig*., Montreal, QC, Canada, pp. 1-3, Mar. 2012.

[15] X.-F. Ye, S.-Y. Zheng, and J.-H. Deng, "A compact patch crossover for millimeter-wave applications," *in Proc. IEEE Int. Workshop Electromagn*., Hsinchu, pp. 1-2, 2015.

[16] Y. L. Zhou, K. Zhou, J. D. Zhang, C. X. Zhou, and W. Wu, "Miniaturized substrate integrated waveguide filtering crossover," *2017 IEEE Electrical Design of Advanced Packaging and Systems Symposium*, Dec. 2017.

[17] S. Y. Zheng and X. F. Ye, "Ultra-compact wideband millimeter-wave crossover using slotted SIW structure," *in Proc. IEEE Int. Workshop Electromagn*., Nanjing, China, pp. 1-2, May 2016.

[18] P. Li, H. Chu, and R. S. Chen, "SIW magic-T with bandpass response," *Electron Lett*., vol. 51, no. 14, pp. 1078-1080, July 2015.

[19] C.-K. Lin and S.-J. Chung, "A compact filtering 180° hybrid," *IEEE Trans. Microw. Theory Tech*., vol. 59, no. 12, pp. 3030-3036, Dec. 2011.

[20] J.-X. Xu, X.-Y. Zhang, and H.-Y. Li, "Compact narrowband filtering rat-race coupler using quad-mode dielectric resonator," *IEEE Trans. Microw. Theory Tech*., vol. 66, no. 9, pp. 4029-4039, Sep. 2018.

[21] Z.-G. Zhang, Y. Fan, and Y.-H. Zhang, "Multilayer half-mode substrate integrated waveguide wide-band coupler with high selectivity," *Appl. Comp. Electro. Society (ACES) Journal*, vol. 34, no. 9, pp. 1418-1425, Sep.2019.

[22] S.-Q. Han, K. Zhou, J.-D. Zhang, C.-X. Zhou, and W. Wu, "Novel substrate integrated waveguide filtering crossover using orthogonal degenerate modes," *IEEE Microw. Wireless Compon. Lett*., vol. 27, no. 9, pp. 803-805, Sep. 2017.

[23] Y.-J. Cheng and Y. Fan, "Compact substrate-integrated waveguide bandpass rat-race coupler and its microwave applications," *IET Microw., Antennas Propag*., vol. 6, no. 9, pp. 1000-1006, June 2012.

[24] H.-Y. Li, J.-X. Xu, and X.-Y. Zhang, "Substrate integrated waveguide filtering rat-race Coupler based on orthogonal degenerate modes," *IEEE Trans. Microw. Theory Techn*., vol. 67, no. 1, pp. 140-150, Jan. 2019.

[25] S. Zhang, J.-Y. Rao, J.-S. Hong, and F.-L. Liu, "A novel dual-band controllable bandpass filter based on fan-shaped substrate integrated waveguide," *IEEE Microw. Wireless Compon. Lett*., vol. 28, no. 4, pp. 308-310, Apr. 2018.

[26] Y.-D. Dong and T. Itoh, "Miniaturized substrate integrated waveguide slot antennas based on negative order resonance," *IEEE Trans. Antennas Propag*., vol. 58, no. 12, pp. 3856-3864, Dec. 2010.

[27] R. Rezaiesarlak, M. Salehi, and E. Mehrshahi, "Hybrid of moment method and mode matching technique for full-wave analysis of SIW circuits," *Appl. Comp. Electro. Society (ACES) Journal*, vol. 26, no. 8, pp. 688-695, Aug. 2011.

[28] Z. J. Zhu, L. Cao, and C. L. Wei, "Novel compact microstrip dual-Mode filters with two controllable transmission zeros," *Appl. Comp. Electro. Society (ACES) Journal*, vol. 33, no. 1, pp. 43-48, Jan. 2018.

[29] J.-S. Hong and M.-J. Lancaster, *Microstrip Filter for RF/Microwave Applications*. New York, NY,

USA: Wiley; 2001.
[30] R.-J. Cameron, "Advanced coupling matrix synthesis techniques for microwave filters," *IEEE Trans. Microw. Theory Tech*., vol. 51, no. 1, pp. 1-10, Jan. 2003
[31] D.-M. Pozar, *Microwave Engineering*. Second edition, New York: Wiley; 1998.

Zhigang Zhang was born in Shanxi Province, China. He received the B.S. degree in Electronic Information Engineering and M.S. degree in Wireless Physics from Sichuan University and is currently working toward the Ph.D. degree in Electro-magnetic Field and Micro-wave Technology from The University of Electronic Science and Technology of China (UESTC), Chengdu, Sichuan, China. His current research interests include SIW technology and its application, microwave and millimeter-wave filters and couplers, electromagnetic theory.

Yong Fan received the B.E. degree from the Nanjing University of Science and Technology, Nanjing, Jiangsu, China, in 1985, and the M.S. degree from the University of Electronic Science and Technology of China (UESTC), Chengdu, Sichuan, China, in 1992.

He is currently with the School of Electronic Engineering, UESTC. He has authored or coauthored over 60 papers. From 1985 to 1989, he was interested in microwave integrated circuits. Since 1989, his research interests include millimeter-wave communication, electromagnetic theory, millimeter-wave technology, and millimeter-wave systems. Fan is a Senior Member of the Chinese Institute of Electronics (CIE).